SCIENTIFIC PERFORMANCE REPORT
OF THE PICsIT INSTRUMENT SPECIFIC SOFTWARE

Version: 1.0 – Date: 28 February 2003
Responsible: Luigi Foschini (IASF–CNR, Sezione di Bologna, Italy)

Summary: This report is to show the scientific performances and reliability of the Instrument Specific Software (ISSW) of the PICsIT detector layer of the IBIS imager. The executables analysed here are those officially delivered to date (28 February 2002), together with their Instrument Configuration (IC) files.

1 What is now available

The PICsIT–ISSW delivered to date for the Scientific Analysis of the PICsIT data include:

- **ibis_pics_deadtime** (v 2.1, 23 October 2002): to calculate the intrinsic deadtime of the detector. It works well; no particular problem after the launch.
- **ip_ev_correction** (v 1.6, 14 November 2002): to perform a correction of gain and offset variations in addition to those performed on board by the Instrument Application Software (IASW). It is for data obtained in photon–by–photon mode. It is strilctly linked with the IC data structure PICS–ENER–MOD, containing the average gain, offset, and the deviations from these values pixel by pixel. The latest version of PICS–ENER–MOD is dated 30 October 2002 and was built by using the data in the IBIS Scientific Performance Report (IBIS Calibration Team, 2002). The exectuable is now stable and working. The only expected changes concerns the IC file, that should be updated with in flight data.
- **ip_ev_shadow_build** (v 2.1, 31 January 2003): to perform the building of the shadowgrams and the efficiency maps from data in photon–by–photon mode. It is stable and working. The only missing part is the treatment of the Good Time Interval (GTI); however, since the photon–by–photon mode is not the standard mode for PICsIT, and it was used only in exceptional cases during the PV phase with dedicated telemetry (because of the high background), the GTI inclusion is a low priority task. The executable is already ready to prepare shadowgrams also for the spectra extraction.
- **ip_si_shadow_build** (v 2.5, 24 February 2003): to perform the building of shadowgrams and the efficiency maps from the data in standard mode (spectral imaging). It is stable and working. It is worth mentioning that the executable select only the complete histograms. If histograms are not complete, the executable returns no shadowgrams. It is foreseen, in the future, to deal also with partially complete histograms. The executable is already ready to prepare shadowgrams also for the spectra extraction.

- **ip_shadow_ubc** (v 2.4, 25 February 2003): to perform the correction for background and detector non–uniformities. The output shadowgrams are also expanded to take into account the gaps between modules. The gaps and the killed pixels are filled with a mean value. There is also a variance map, calculated starting from the statistical variance of the detector counts and updated according to the correction performed. The executable is linked with the following IC data structures: PICS–SBAC–BKG (background maps for single events), PICS–MBAC–BKG (background maps for multiple events), PICS–SUNI–BKG (detector non–uniformities for single events), and PICS–MUNI–BKG (detector non–uniformities for multiple events). See Sect. 2 for details.

- **ip_skyimage** (v 2.2, 25 February 2003): it performs the deconvolution and sky image reconstruction by means of the algorithm described by Goldwurm et al. (2001). The executable is working, producing a basic deconvolved sky image, variance, and significance maps. See Sect. 3 for details.

- **ip_st_lc_extract** (v 2.0, 23 February 2003): it performs the extraction of the lightcurve of the whole detector from the spectral timing data. The barycentric correction is applied, by using the library DAL3AUX. The executable is working.

- **Additional notes**: The executable for the Automatic Calibration Analysis (ACA) is not yet completed, because it is necessary to wait for an analysis of in–flight variations of the gains. After this analysis, it will be decided if this executable is necessary or not. The executables for the extraction of the spectrum and lightcurves from point–like sources are not yet ready. Work is in progress.

More details on some single items are in the following sections.

2 The background correction

There are no detector non–uniformities map available to date, except of one map created for test purposes (single events; no energy selection). The map is not to be used with the actual version of the ISSW, since it has been written with an old template, no more used. Using this map, can give wrong results and the crash of the pipeline. The removal of these maps from the archive has been requested.

For the background maps, the situation is different: there are three useful sets, prepared from the empty field observations of the revolution 13 (1 set for single and multiple events; 8 energy bands) and 38 (2 sets for single and multiple events; 8 energy bands). The differences in the two sets from the revolution 38 are due to a change in the energy bands.

PICsIT operates in an energy region dominated by the background, where we expect that the source counts are of the order of 1% of the global counts detected.

This means that the background subtraction is of fundamental importance for the detection capabilities.

The availability to date of only the empty field observations does not allow the user to be free to select the energy bands to produce images. A set of default energy bands has been created to have the best source statistics, with the lowest possible contamination from background or other events, such as the cosmic–rays induced events (see Segreto 2002). These energy bands, prepared by G. Di Cocco and G. Malaguti, are shown in Table 1.

Table 1: PICsIT Energy Bands. Columns: (1) Channel number in photon–by–photon mode; (2) Channel number in standard mode; (3) Energy [keV].

Channels PPM (1)	Channels Standard (2)	Energy (3)
Single Events		
29 – 35	10 – 16	203 – 252
36 – 46	17 – 27	252 – 329
47 – 64	28 – 41	329 – 455
65 – 94	42 – 56	455 – 655
95 – 150	57 – 84	655 – 1057
151 – 262	85 – 140	1057 – 1841
263 – 509	141 – 196	1841 – 3570
510 – 929	197 – 254	3570 – 6510
Multiple Events		
24 – 31	5 – 12	336 – 448
32 – 46	13 – 27	448 – 658
47 – 74	28 – 46	658 – 1050
75 – 130	47 – 74	1050 – 1834
131 – 254	75 – 136	1834 – 3570
255 – 464	137 – 187	3570 – 6510
465 – 679	188 – 229	6510 – 9520
680 – 929	230 – 254	9520 – 13020

A set of background maps corresponding to the energy bands listed in Table 1 have been created. No corresponding detector uniformity maps have been created, since a modelling activity is necessary to separate the contribution of the background from the detector non–uniformities. With the empty field observations is only possible to subtract the background. Nevertheless, this correction, although partial, is sufficient.

It is worth mentioning, as already seen in SIGMA calibrations and data reduction (Bouchet et al. 2001), that a background subtraction is more efficient when the background map is prepared from a nearby observation. This means that the background map generation is continuosly evolving. In addition, studies are necessary to develop a parametric model, that will result also in giving to the user the possibility to freely select the energy bands.

Actually the executable contains two ways to rescale the background maps: according to the time of exposure and to the average value of counts. Although a more detailed study is necessary, it appears that the average value scaling could give better results in searching for weak sources. However, this is still to

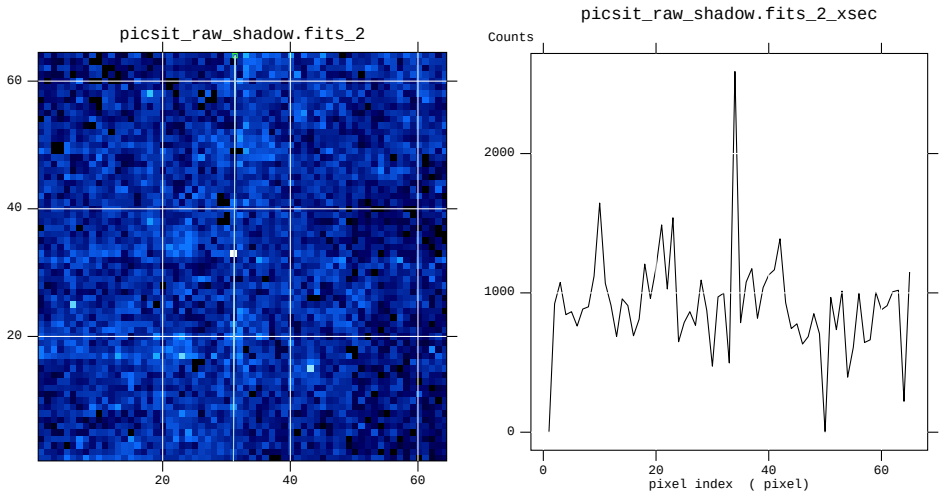

Figure 1: Effect of cosmic-rays induced events on the shadowgrams. The white pixels have an anomalous high count value.

be validated.

An *a posteriori* correction for the cosmic–rays induced events (see Segreto 2002) is also performed: when the pixel counts are higher than a constant multiplied by the average count values, i.e. $counts > k \cdot average$ (see Fig. 1), then it is assumed that this abnormal high value is due to a cosmic–ray induced event and the pixel value is reset to the mean value. First tests showed a certain effectiveness of this correction, but work is in progress to have a better solution, according to the casual nature of these events.

3 The sky image reconstruction

3.1 Efficiency of the deconvolution

One of the most important points in the restoring of the sky image is the decoding pattern. The mask and the detector grid have different pitches: the mask is spaced by 11.2 mm, while the PICsIT pixel pitch is 9.2 mm. According to the type of algorithm used, it could be necessary to interpolate the decoding pattern obtained from the mask to the detector grid or *vice–versa*.

In the actual algorithm implemented in the PICsIT module, the decoding pattern is interpolated on the detector grid: in this way, we can save computer processing time. The interpolation is performed once, stored in an IC file (PICS–DECO–MOD), and loaded when necessary.

The selected interpolation has a great impact in the efficiency of the deconvolution and several interpolation algorithms are now under study to select the best choice. The actual delivered version is based on a simple bilinear interpola-

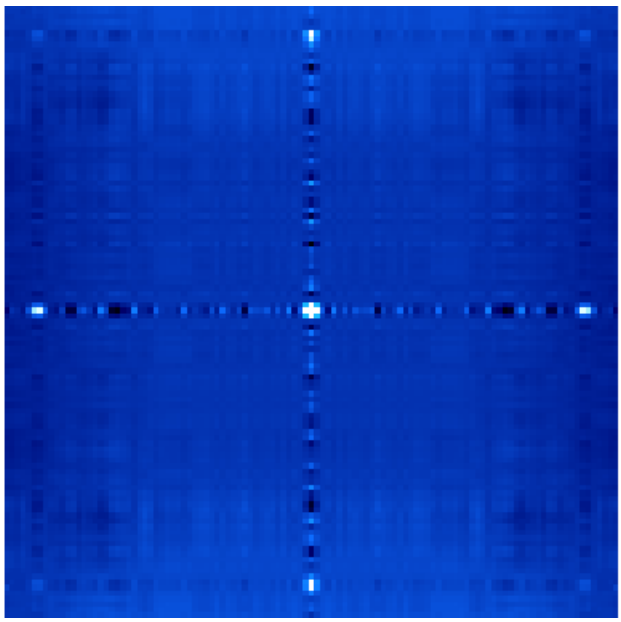

Figure 2: Point Spread Function of PICsIT with the decoding pattern interpolated with bilinear interpolation.

tion and appears to give good and reliable results, as shown by the Point Spread Function in Fig. 2. With the actual hardware characteristics (mask and detector grid, etc...) the maximum significance in the PSF with a perfect interpolation is $\sigma \approx 47$; the actual available reaches $\sigma \approx 37$, corresponding to an efficiency of the deconvolution of about 79%. Work is in progress to improve the efficiency.

3.2 Sky coordinates reconstruction

The sensitivity of PICsIT does not allow to see sources during a typical exposure of one ScW ($2 - 5$ ks). It is necessary to integrate the shadowgrams to obtain long exposures of the order of $10^4 - 10^5$ s. This resulted to be problematic in realizing a detailed and extensive study of misalignement. To date, only two sources are available to test the sky coordinates reconstruction: they are the Crab – in the FCFOV – and GRB021125 – in the PCFOV – (Bazzano and Paizis 2002).

The position of the Crab can be checked with the known catalog position, e.g. Simbad. For the GRB there can be the problem that the only position available with sufficient precision is that obtained with ISGRI (Gros and Produit 2002), the low–energy detector layer of IBIS, and there is the risk of self–reference. But the follow–up with other satellites of the GCN (GRB Coordinates Network) confirmed the position.

In the Table 2 are reported the positions found and the comparison with the other known coordinates. It is worth mentioning that one pixel of PICsIT corresponds to about $12'$, so that an offset of $6.7'$ corresponds to about half a pixel. In addition, this is the position after a basic deconvolution: it is foreseen to add a gaussian smoothing of the source to fit the peak, so to have a better positioning. The remaining offset will be corrected by using the misalignement matrix.

Table 2: Source position accuracy. Columns: (1) Source name; (2) Reference position (RA, Dec, J2000) from catalog or circulars; (3) PICsIT position (RA, Dec, J2000); (4) Offset [arcmin].

Source	Reference Position	PICsIT Position	Offset
(1)	(2)	(3)	(4)
Crab	$05:34:32; +22:00:52$	$05:34:13; +21:55:48$	$6.7'$
GRB021125	$19:47:56, +28:23:28$	$19:47:13, +28:15:13$	$9.6'$

It has been noted a little additional shift in the position of the Crab when detected at the highest energies, probably due to the increase of the mask transparency and, therefore, the coding is not complete.

4 The performances with the Crab on axis

4.1 Imaging

The second part of the PV phase has been performed during February 2003. During the revolution 38 there were observations of empty field, useful for the background subtraction. Actually only about 13 ks (single events) and less than 9 ks (multiple events) of empty field observations were available and used to produce background maps (see Sect. 2).

Table 3: PICsIT observations of the Crab during Rev. 39. Columns: (1) Energy band [keV]; (2) Count rate in the peak pixel [c/s]; (3) Significance of the detection.

Energy Band	Rate	σ
(1)	(2)	(3)
$170 - 200$	2.8	7.4
$200 - 250$	2.8	10.5
$250 - 300$	1.7	11.4
$300 - 350$	1.0	7.8
$350 - 400$	0.6	6.4
$400 - 2000$	1.9	8.1
$2000 - 4700$	–	–
$4700 - 7200$	–	–

For the analysis with the Crab were selected about 21 ks of data from the staring observation during the revolution 39 (PICsIT in standard mode). The

results are shown in the Table 3. They can be compared with the Monte Carlo simulations by Del Santo et al. (2001), although simulations were done in different energy bands. M. Del Santo (2003, private communication) calculated the proper values of expected count rates in three energy bands comparable with the results of the ISSW (Table 4).

Table 4: PICsIT observations of the Crab. Comparison of real data from ISSW and Monte Carlo simulations. Columns: (1) Energy band of real data [keV]; (2) Count rate [c/s]; (3) Energy band of simulations [keV]; (4) Count rate [c/s].

Energy Band (1)	Rate (2)	Energy band (3)	Rate (4)
$170 - 250$	5.6	$150 - 250$	10
$250 - 400$	3.3	$250 - 400$	4.6
$400 - 2000$	1.9	$400 - 1000$	2.1

These results are also confirmed by a software for the PICsIT imaging developed independently in Bologna by J.B. Stephen and running on the same data structure (G. Di Cocco, personal communication, 2003).

In the Fig. 3, is is shown the significance map of the observation at $250 - 300$ keV, the best detection, together with the radial profile. In the Fig. 4–6 are shown all the other significance maps corresponding to the detections listed in Table 3. The color scale has been selected to emphasize the detections.

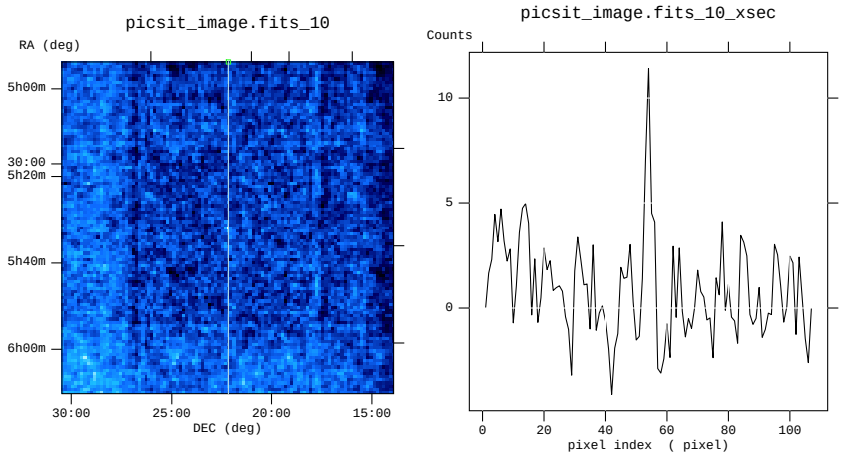

Figure 3: PICsIT significance map and radial profile of the Crab observation in the energy band $250 - 300$ keV.

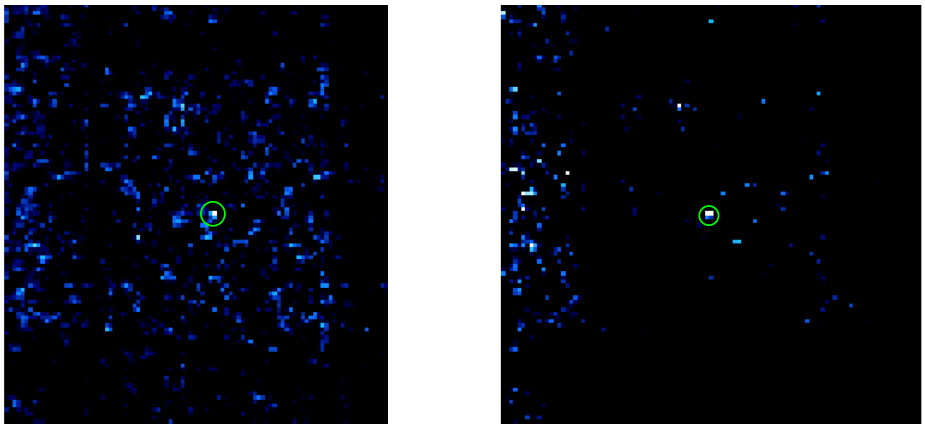

Figure 4: PICsIT significance map of the Crab observation in the energy band $170 - 200$ keV (left) and $200 - 250$ keV (right).

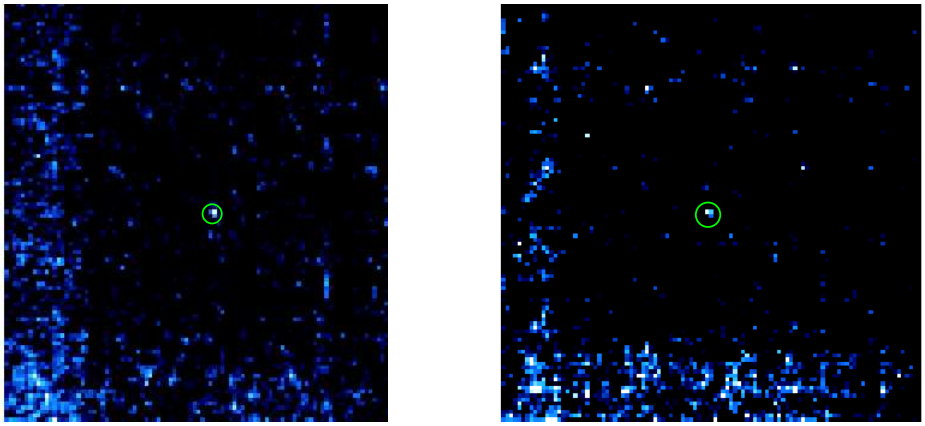

Figure 5: PICsIT significance map of the Crab observation in the energy band $250 - 300$ keV (left) and $300 - 350$ keV (right).

4.2 Timing

In the Rev. 41, when the Crab was off–axis, PICsIT was in standard mode with the spectral timing set at about 1 ms of time resolution and four energy bands. The files obtained are very huge and it was not possible to analyze more than 2 Scw for problems of disk space. Nevertheless, a first weak detection of the period of the Crab is visible (Fig. 7). According to the Jodrell Bank monthly ephemeris of the Crab pulsar, the period is 0.03354548462 s measured on 15 January 2003. The best period found by PICsIT ISSW on a timescale of 2 Scw

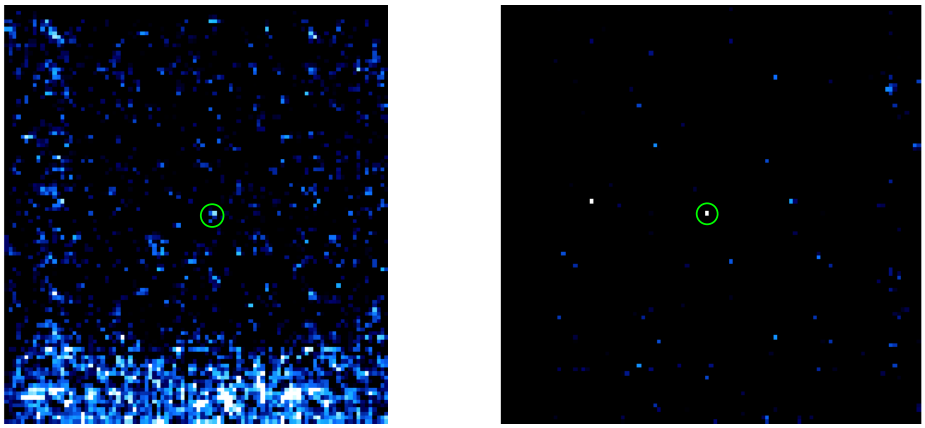

Figure 6: PICsIT significance map of the Crab observation in the energy band $350 - 400$ keV (left) and $400 - 2000$ keV (right).

(exposure 8634 s) is 0.033548678 s, with some offset of the order of -10^{-6} s. Being the time resolution of 1 ms, this means that the differences found are at level of "numerical noise".

The detection is weak and it is expected to have better results with longer observations. Nevertheless, the ISSW appears to work. It is worth noting that actually the barycentric correction is implemented, but not yet fully tested. Work in progress.

5 Additional tools

5.1 OSM

There are also three executables for the Operating Status Monitoring (OSM) in standard mode (spectral imaging, spectral timing) and photon–by–photon mode. They produce some standard products to monitor the instrument performances, that is shadowgrams, spectra and lightcurves for the whole detector, statistical analysis on the shadowgrams (mean value, maximum, minimum, standard deviation). They are all working and stable. They are already used for the Consolidated Data Processing.

5.2 Background maps

An executable was developed to generate the background maps from empty field observations. Although, it is not intended for the common user, it is developed following the ESA and ISDC Coding and Testing Standards, so that, if necessary, it can be integrated in the usual ISDC pipelines. The executable is stable and

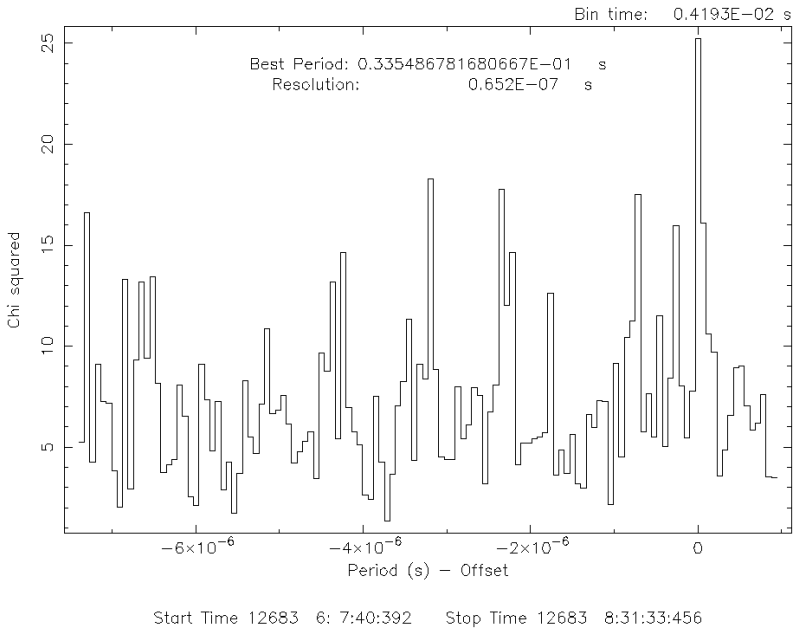

Figure 7: Best period found for the Crab from 2 Scw of spectral timing data. Energy band: $208 - 260$ keV.

working fine. The background maps available in the IC data base have been generated by means of this executable.

6 Non–standard analysis tools

In some particular cases, like the detection of GRB when PICsIT is in photon–by–photon mode, it could be necessary to extract the data with non–standard procedures. In normal conditions this is not possible. Indeed, by taking into account that PICsIT will work for almost its "life" in standard mode, a GRB of tens of seconds will be lost in an histogram of thousands of seconds. But, if PICsIT is in photon–by–photon mode, it is possible to extract the photon list of a selected time region and to perform the scientific analysis. While for imaging it is possible to use the usual executable (ip_skyimage), the extraction of the spectrum and the lightcurve requires a dedicated software. Some tools have been developed for the analysis of the GRB021125 (Bazzano and Paizis 2002), the first GRB seen by IBIS, during which PICsIT was in photon–by–photon.

The GRB has a high throughput of photons for a very short time and it well surpass the background count rate (see the lightcurve of the whole detector in Fig. 8). So that, if we consider the photons of the whole detector when observing the GRB and we subtract the background from an empty field observation, it

is possible to extract a spectrum of the GRB (Fig. 8, up). The results obtained with the GRB021125 have been compared with those obtained by IBAS both for ISGRI and SPI–ACS, with the help of G. Malaguti, S. Mereghetti, J. Borkowski, and D. Götz. Results are consistent.

Two exectuables have been developed for this purpose and even though they are not intended for the standard pipeline, they are already suitable to became available for the users, since they are developed following the ESA and ISDC Coding and Testing Standards.

7 Final remarks

The latest executables delivered up to date are the basis for a stable, although basic, pipeline for the PICsIT scientific analysis. First tests, comparison with other software and Monte Carlo simulations show that the data products are reliable from a scientific point of view.

It is clear that there is still a lot of work to do: improvements in the data products, prototyping of algorithms, search for test cases, and so on. However, it appears that the first good results are coming.

References

[1] Bazzano A., Paizis A., 2002, GCN1706

[2] Bouchet L. et al., 2001, ApJ 548, 990.

[3] Del Santo M. et al., 2001, AIP Conference Proceedings **587**, 826.

[4] Goldwurm A. et al., 2001, Proceedings of the IV INTEGRAL workshop, ESA **SP–459**, p. 497.

[5] Gros A., Produit N., 2002, GCN1714

[6] IBIS Calibration Team, *Scientific Performance Report*, IN.IB.IAS.RP.008/02, March 2002.

[7] Segreto A., *The cosmic–ray induced events on PICsIT*, IN.IB.IASF/Pa.RP.030/02, November 2002.

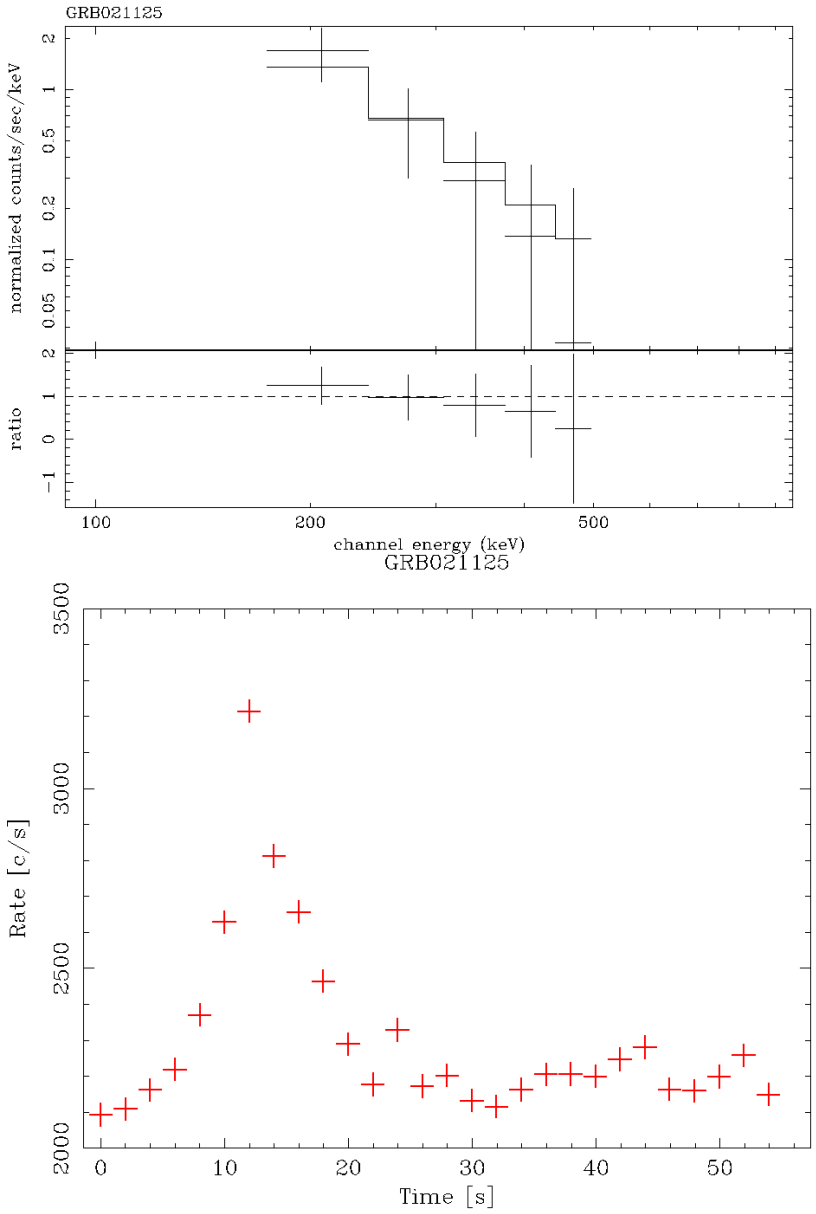

Figure 8: GRB021125: spectrum (up) and lightcurve (down) produced with non–standard analysis. The spectrum is in the band 200−500 keV and convolved with the best response matrix available to date. The lightcurve is rebinned with 2 s intervals.